Mineralogical Magazine (2022), **86**, 205–213
doi:10.1180/mgm.2022.9

CAMBRIDGE UNIVERSITY PRESS

Article

Gachingite, $Au(Te_{1-x}Se_x)$ $0.2 \approx x \leq 0.5$, a new mineral from Maletoyvayam deposit, Kamchatka peninsula, Russia

Nadhezda D. Tolstykh[1], Marek Tuhý[2,3]*, Anna Vymazalová[2], František Laufek[2], Jakub Plášil[4] and Filip Košek[3]

[1]VS Sobolev Institute of Geology and Mineralogy of SB RAS, prosp. Akademika Koptyuga, 3, 630090, Novosibirsk, Russia; [2]Czech Geological Survey, Geologická 6, 152 00 Prague 5, Czech Republic; [3]Institute of Geochemistry, Mineralogy and Mineral Resources, Faculty of Science, Charles University, Albertov 6, 128 00 Prague; and [4]Institute of Physics ASCR, v.v.i., Na Slovance 2, 128 21 Prague 8, Czech Republic

Abstract

Gachingite, $Au(Te_{1-x}Se_x)$, $0.2 \approx x \leq 0.5$, is a new mineral discovered in the Gaching ore occurrence of the Maletoyvayam epithermal deposit, Kamchatka, Russia. Gachingite forms individual droplet-like grains of sizes from 2 to 10 μm included in native gold (Au–Ag), associated with calaverite, maletoyvayamite, watanabeite and Au–Sb oxides. The aggregates do not exceed 100 μm in diameter. In plane-polarised light, gachingite is grey with a bluish tint, has bireflectance (bluish-grey to deep grey), and strong anisotropy with rotation tints blue to dark blue to brown. Reflectance values for gachingite in air (R_{min}, R_{max} in %) are: 39.9, 40.3 at 470 nm; 41.6, 43.3 at 546 nm; 42.0, 43.7 at 589 nm; and 43.0, 44.0 at 650 nm. Eighteen electron-microprobe analyses of gachingite gave an average composition: Au 62.40, Ag 0.57, Se 9.78, Te 27.33 and S 0.01, total 100.09 wt.%, corresponding to the formula $(Au_{0.96}Ag_{0.02})_{\Sigma 0.98}(Te_{0.65}Se_{0.37})_{\Sigma 1.02}$ based on 2 apfu, the simplified formula is $Au(Te_{0.65}Se_{0.35})$; the average analyses of its synthetic analogue is Au 65.7, Se 13.1 and Te 21.1, total 99.9 wt.%, corresponding to $Au_{1.00}(Te_{0.50}Se_{0.50})$. The calculated density is 10.47 g/cm^3. The mineral is orthorhombic, space group *Cmce* (#64) with $a = 7.5379$ Å, $b = 5.7415$ Å, $c = 8.8985$ Å, $V = 385.12$ Å^3 and $Z = 8$. The crystal structure was solved and refined from the single-crystal X-ray-diffraction data of synthetic $Au_{1.00}(Te_{0.50}Se_{0.50})$. The crystal structure of gachingite represents a unique structure type, containing linear [Au–Au–Au] chains running along the **b**-axis indicating strong metallic interaction in one direction. The structural identity of gachingite and its synthetic analogue $Au_{1.00}(Te_{0.50}Se_{0.50})$ was confirmed by electron back-scatter diffraction and Raman spectroscopy. The formation of gachingite requires an abundant source of Au and Se and a high oxidising environment. Gachingite is related to the gold-bearing productive stage of ore mineralisation, which is stable at 250°C in $\log f_{Se_2}$ range of −12.4 and −5.7. The mineral is named after its type locality.

Keywords: gachingite, $Au(Te_{1-x}Se_x)$ phase, reflectance data, chemical composition, X-ray-diffraction data, crystal structure, Gaching, Maletoyvayam deposit, Kamchatka, Russia

(Received 22 November 2021; accepted 18 January 2022; Accepted Manuscript published online: 24 January 2022; Associate Editor: Irina O Galuskina)

Introduction

The polished section that contains grains of gachingite $Au(Te_{1-x}Se_x)$, $0.2 \approx x \leq 0.5$, comes from the Gaching ore occurrence of the Maletoyvayam deposit, located in the southwestern part of the Koryak Highland of the central Kamchatka volcanic belt, Far East, Russia (60°19′51.87″N, 164°46′25.65″E). Gold-rich aggregates containing gachingite were obtained by crushing mineralised rocks and panning the resulting material into a heavy fraction using hydroseparation, followed by concentration using heavy liquids. Gachingite was found in polished sections made from the heavy mineral concentrate, which was obtained from a 20 kg sample of alunite–quartz rock. Gachingite was found in the same material as the recently described mineral maletoyvayamite (Tolstykh *et al.*, 2020).

Both the mineral and its name (symbol Gac) were approved by the Commission on New Minerals, Nomenclature and Classification of the International Mineralogical Association (IMA2021-008, Tolstykh *et al.*, 2021). The name gachingite (Cyrillic – гачингит) is after its type locality, the Gaching occurrence of the Maletoyvayam deposit in the Kamchatka peninsula, Russia.

Holotype material with gachingite (polished section) and its synthetic analogue (Exp AU4) are deposited in the Central Siberian Geological Museum (CSGM) of the VS Sobolev Institute of Geology and Mineralogy of the Siberian Branch of the Russian Academy of Sciences (IGM SB RAS), Novosibirsk, Russia, catalogue number V–10/1.

Occurrence

The Maletoyvayam deposit, like most of the Au–Ag deposits of the Kamchatka Peninsula, is located in the Oligocene–

*Author for correspondence: Marek Tuhý, Email: marek.tuhy@geology.cz
Cite this article: Tolstykh N.D., Tuhý M., Vymazalová A., Laufek F., Plášil J. and Košek F. (2022) Gachingite, $Au(Te_{1-x}Se_x)$ $0.2 \approx x \leq 0.5$, a new mineral from Maletoyvayam deposit, Kamchatka peninsula, Russia. *Mineralogical Magazine* **86**, 205–213. https://doi.org/10.1180/mgm.2022.9

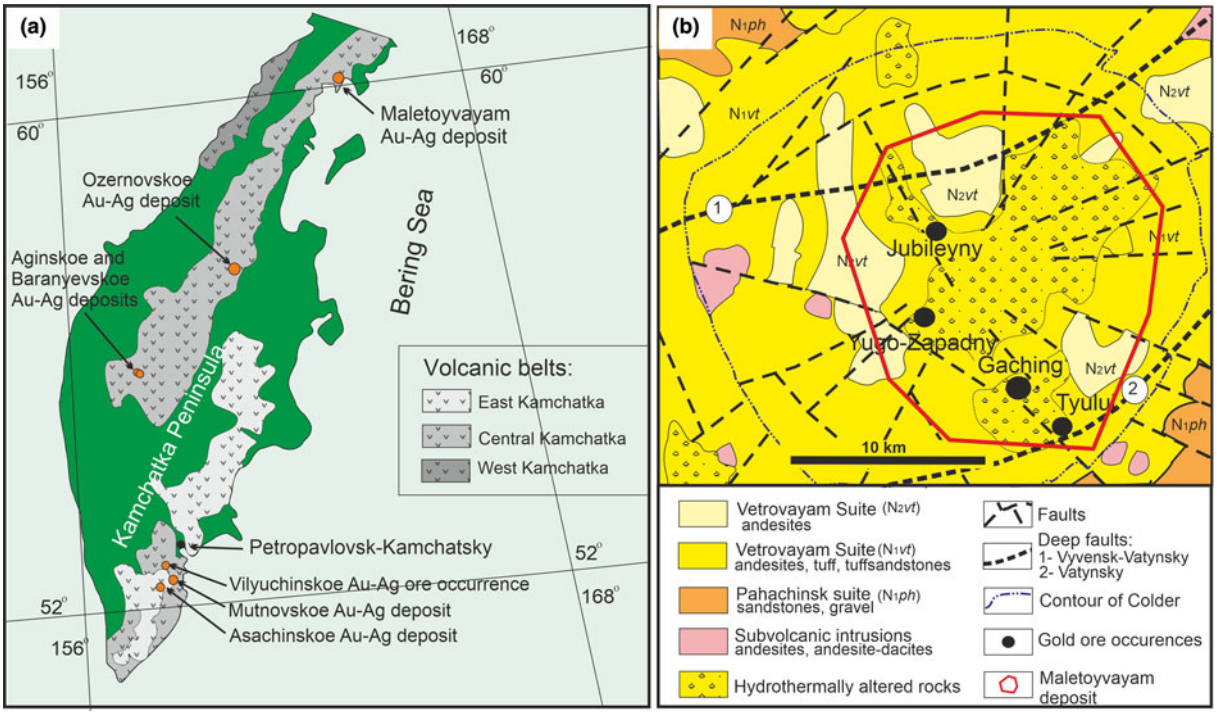

Fig. 1. (a) Location of Au–Ag deposits (Okrugin *et al.*, 2017) within the volcanic belts (Tsukanov, 2015) in the Kamchatka Peninsula; and (b) geological map of the Maletoyvayam deposit modified after Lyashenko and Mikhaylova (1972).

Quaternary Central Kamchatka volcanic belt, which extends along the direction of the modern subduction trend (Okrugin *et al.*, 1994; Khanchuk and Ivanov, 1999). All Au–Ag deposits located in this belt: Ozernovskoe, Aginskoe, Baranyevskoe, Asachinskoe, Rodnikovoe etc (Fig. 1a), except for the Maletoyvayam deposit, belong to the epithermal low-sulfidation (LS) type with a wide development of near-surface mineralisation of the telluride subtype (Takahashi *et al.*, 2002, 2007; Goryachev *et al.*, 2010; Okrugin *et al.*, 2015). The Maletoyvayam deposit is located in the southwestern part of the Koryak Upland (Melkomukov *et al.*, 2010) in the Vetrovayam volcanic zone and is hosted by the rocks of Vetrovayam Suite (andesites, tuff and tuffsandstones). It is the only Au–Ag deposit known in Kamchatka that belongs to the epithermal high-sulfidation (HS) type (Tolstykh *et al.*, 2018; Sidorov *et al.*, 2020). The Maletoyvayam deposit combines four ore occurrences in the ore field: Gaching, Yubileyny, Yugo-Zapadny and Tyulul (Fig. 1b). The main gangue minerals are quartz, alunite, native sulphur and kaolinite. Vuggy silica was identified in the central part of the ore field, transitioning outwards into quartz–alunite, quartz–kaolinite, quartz–sericite–kaolinite and then to argillic- and propylitic-altered rocks (Melkomukov *et al.*, 2010). The Gaching ore occurrence, in which the minerals maletoyvayamite and gachingite were found, is located at the head of the Gachingalhovayam River.

The Maletoyvayam deposit, specifically the Gaching occurrence, differs from other epithermal deposits in Kamchatka by having a significant mineral variety. Native high-grade gold, including the hypergene mustard gold, is not dominant in these ores, whereas Au and Ag chalcogenides, Cu–Sb–As–Te sulfosalts, as well as complex metastable Au-containing oxides, and other associated rare or unique phases are the most common (Tolstykh *et al.*, 2017, 2018, 2019, 2020; Shapovalova *et al.*, 2019; Sidorov *et al.*, 2020). A mineral having a similar composition to gachingite was described as an unnamed phase Au(Te,Se) by Tolstykh *et al.* (2018). It should be noted that such a compound has never been found before in any other epithermal deposit. Such unique compounds require special conditions for their formation: an abundant source of Au and Se and a high oxidising environment. Gachingite, embedded in gold, is related to the gold-bearing productive stage of ore mineralisation, which is stable at 250°C in $\log f_{Se_2}$ range of −12.4 and −5.7. A further increase of f_{O_2} leads to oxidation of Au-tellurides to Au–Ag–(Sb,As,Te,S) oxides and the formation of mustard gold (Tolstykh *et al.*, 2018, 2019). Thermometric studies of fluid inclusions in quartz showed that the range of conditions during the formation of the gold-bearing productive stage are: fluid inclusions salinity of 4.3 wt.% NaCl eq, temperature of 255–245°C, and pressure of 39–32 bar (Sidorov *et al.*, 2020).

Appearance, physical and optical properties

Gachingite forms individual droplet-like grains of sizes from 2 to 10 μm embedded in native gold (Au–Ag), in association with calaverite, maletoyvayamite, watanabeite and Au–Sb oxides. The aggregates do not exceed 100 μm in diameter. Reflected light and back-scattered electron images of the described mineral are shown in Fig. 2.

Gachingite is opaque, brittle, with a metallic lustre. The density calculated on the base of the empirical formula is 10.47 g/cm^3. In plane-polarised reflected light, gachingite is grey with a bluish tint, has strong bireflectance, strong anisotropy with rotations tints blue to dark blue to brown. It exhibits no internal reflections.

Reflectance was measured in the air relative to a WTiC standard using Zeiss 370; spectrophotometer MSP400 TIDAS mounted to Leica microscope, objective 50× (National Museum in Prague, Czech Republic). Data are given in Table 1 and plotted in Fig. 3.

https://doi.org/10.1180/mgm.2022.9 Published online by Cambridge University Press

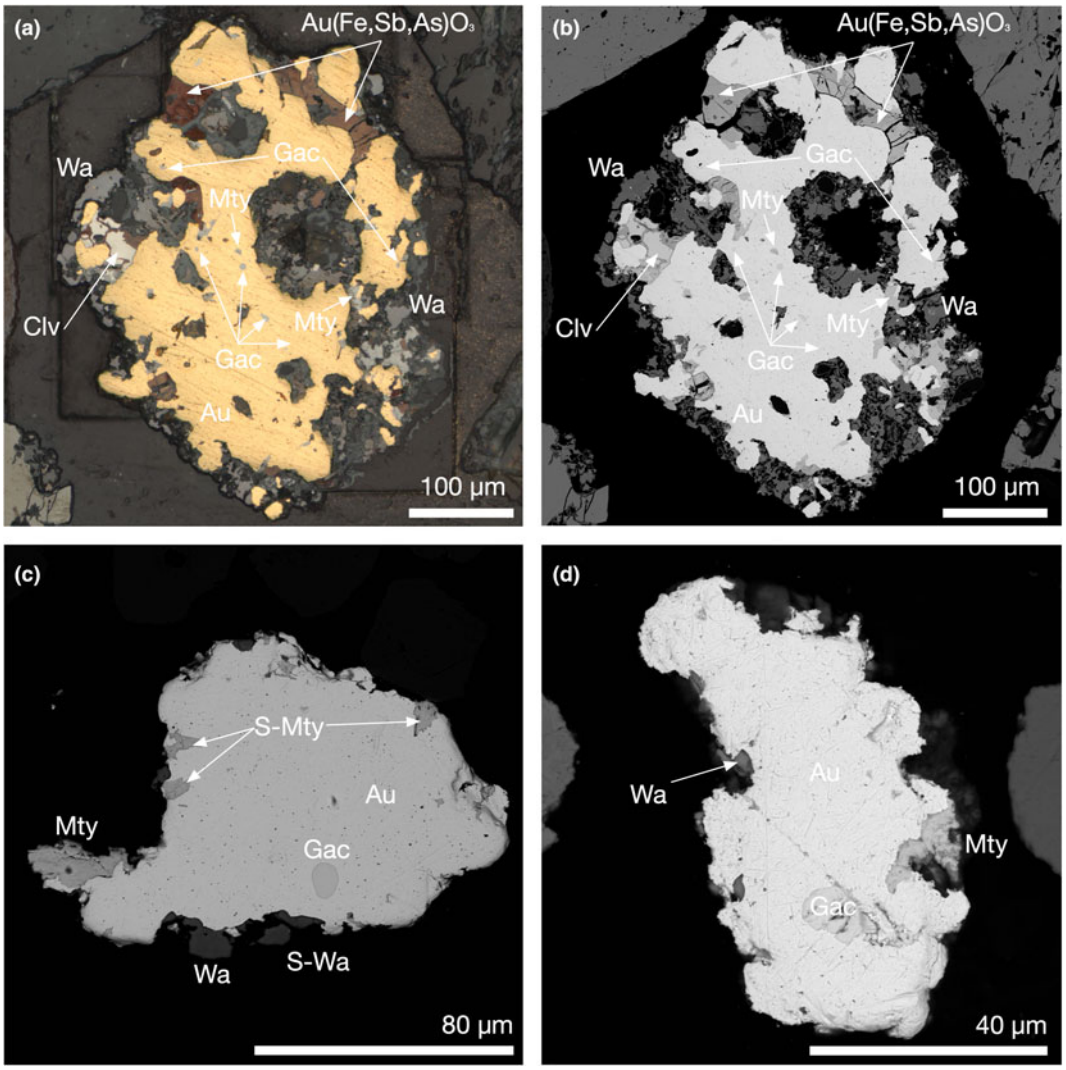

Fig. 2. Images of gachingite (Gac) in association with maletoyvayamite (Mty), watanabeite (Wa), calaverite (Clv) and Au(Fe,Sb,As)O_3 included in native gold. (a) Reflected light; (b–d) back-scattered electron images.

Synthetic analogue

The small size of gachingite grains (2 to 10 µm) and its intergrowths with gold prevented its extraction and direct investigations by means of X-ray diffraction. Therefore, the relevant crystallographic and structural investigations were performed on the synthetic analogue of gachingite $Au_{1.00}(Te_{0.50}Se_{0.50})$.

Table 1. Reflectance data for gachingite.*

R_{max}	R_{min}	λ (nm)	R_{max}	R_{min}	λ (nm)
39.2	37.7	400	43.5	41.7	560
40.8	39.5	420	43.7	41.2	580
40.9	40.2	440	**43.7**	**42.0**	**589**
40.2	40.0	460	43.9	42.2	600
40.3	**39.9**	**470**	43.8	42.4	620
40.4	39.9	480	44.0	42.8	640
41.2	40.4	500	**44.0**	**43.0**	**650**
42.3	41.6	520	44.1	43.2	660
43.1	41.4	540	44.4	43.8	680
43.3	**41.6**	**546**	44.8	44.3	700

*The values required by the Commission on Ore Mineralogy are given in bold.

The synthetic $Au_{1.00}(Te_{0.50}\ Se_{0.50})$ phase was prepared using the evacuated silica glass tube method in the Laboratory of Experimental Mineralogy of the Czech Geological Survey in Prague. Gold (99.95%; additionally, refined at the laboratory using the digestion-precipitation technique), tellurium (99.999%) and selenium (99.999%) were used as starting materials for the synthesis. The evacuated silica-glass tube with its charge was sealed and heated at 400°C. Three times during the experiment, after cooling by cold-water bath, the charge was ground into powder in acetone using an agate mortar and mixed thoroughly to homogenise. The pulverised charge was sealed in an evacuated silica-glass tube again and heated at 400°C for four months. Finally, the experimental product was quenched rapidly in a cold-water bath.

Chemical composition

The electron probe microanalyses data of gachingite were obtained using a JEOL JXA–8230 microprobe (beam size ≈ 1 mm) at 20 kV and 50 nA at the Analytical Center for Multi-Elemental and Isotope Research at the VS Sobolev Institute of Geology and Mineralogy SB RAS (IGM SB RAS) in Novosibirsk, Russia

https://doi.org/10.1180/mgm.2022.9 Published online by Cambridge University Press

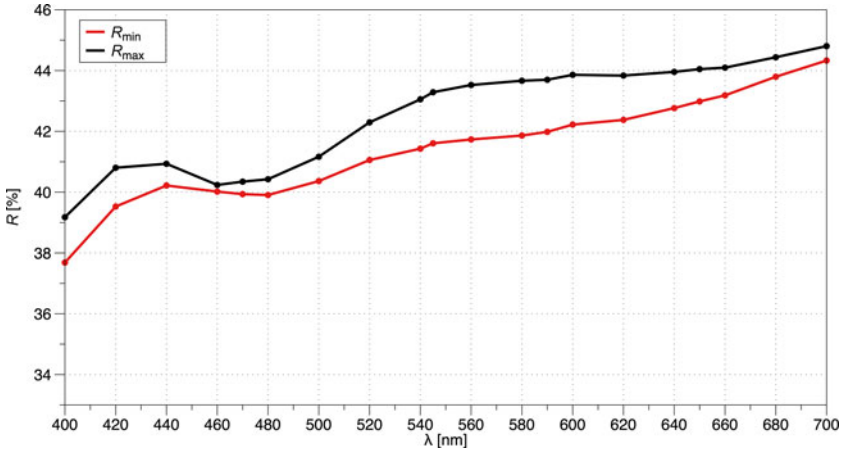

Fig. 3. Reflectance data for gachingite.

(analyst V. Korolyuk). The following X-ray lines (and standards) were used: Se*Lα* (Bi_2Se_3), Te*Lα* ($AgTe_2$), Ag*Lα* (Ag), S*Kα* ($CuFeS_2$) and Au*Mα* (Au). These results were processed using ZAF correction. Values of the minimum detection limit are <0.05% for all the elements analysed. The accuracy and reproducibility of the analytical procedures were evaluated with special tests (Lavrent'ev *et al.*, 2015). Additional data were collected on the Tescan Mira3 GMU equipped with a wavelength dispersion spectrometers (WDS) spectrometer (based at the Czech Geological Survey) under the conditions of 15 kV accelerating voltage and beam current of 8.7 nA.

A synthetic analogue of gachingite was examined using an electron probe microanalyser (EPMA, CAMECA SX-100) equipped with WDS. Quantitative data and chemical analysis were obtained using 15 kV acceleration voltage and 10 nA beam current (diameter: 1–2 μm). For Au and Te calibration, pure metals were used. Selenium was calibrated using Bi_2Se_3 and S using FeS_2. No other elements with atomic numbers higher than eight were detected.

Preliminary analyses of gachingite and associated minerals were also examined using a LEO-413VP scanning electron microscope with INCA Energy 350 microanalysis system (Oxford Instruments Ltd., Abingdon, UK) equipped with EDS (analyst M. Khlestov) at IGM SB RAS. The operating conditions were: an accelerating voltage of 20 kV, beam current of 0.4 nA, 50 s measuring time and beam diameter of ~1 μm.

The EPMA data of gachingite and its synthetic analogue are given in Table 2. The composition of gachingite shows a limited solid solution from $Au(Te_{0.5}Se_{0.5})$ to $Au(Te_{0.8}Se_{0.2})$. EPMA data of gachingite are plotted in the Au–Te–Se diagram in Fig. 4. The empirical formula, calculated for the mean composition ($n = 18$; measured on 7 different grains) on the basis of the sum of all atoms is equal to 2 atoms per formula unit (apfu) is $(Au_{0.96}Ag_{0.02})_{\Sigma 0.98}(Te_{0.65}Se_{0.37})_{\Sigma 1.02}$ for gachingite, the simplified chemical formula is $Au(Te_{1-x}Se_x)$ with the range $0.2 \approx x \leq 0.5$.

X-ray crystallography

A fragment 17 μm × 12 μm × 7 μm of synthetic $Au_{1.00}(Te_{0.50}Se_{0.50})$ was mounted on a glass fibre and examined using a Rigaku Super Nova single-crystal diffractometer with an Atlas S2 CCD detector utilising monochromatised Mo*Kα* radiation from the microfocus X-ray tube. The ω rotation scans were used for the collection of three-dimensional intensity data. From 1109 reflections, 229

Table 2. Chemical composition of gachingite (wt.%) and its synthetic analogue.*

Natural gachingite (wt.%)						
Grain code	Se	Te	S	Au	Ag	Total
G-1C 3_5	6.80	30.67		62.64	0.46	100.57
G-1D 12_12	8.47	28.96	0.03	62.11	0.27	99.84
G-1D 12_16	8.66	28.63	0.01	62.08	0.27	99.65
G-1D 12_11	8.74	28.72	0.01	62.15	0.30	99.92
G-1D 12_13	8.90	28.71	0.02	62.17	0.27	100.07
G-1D 12_15	8.91	28.59	0.01	62.15	0.30	99.96
G-1D 12_14	8.96	28.61	0.01	62.02	0.30	99.90
G-1C 3_3	10.12	27.34	0.01	63.93	0.82	102.22
G-1C 3_1	10.21	27.13	0.01	63.46	0.86	101.67
G-1C 3_6	13.46	22.60	0.01	65.15	0.54	101.76
2a	6.45	31.53		62.17	0.56	100.71
2b	6.37	31.51		60.63	0.62	99.13
3a	9.84	27.72		61.46	0.74	99.76
3b	9.83	27.52		61.37	0.65	99.37
4a	12.64	23.07		61.78	0.95	98.44
4b	12.86	23.44		61.62	0.98	98.90
6a	12.30	23.49		62.30	0.67	98.76
6b	12.44	23.72		64.08	0.73	100.97
Average	9.78	27.33	0.01	62.40	0.57	100.09
Synthetic analogue (wt.%)						
(mean; $n = 6$)	13.11	21.09		65.70		99.90
Natural gachingite (apfu)						
	Se	Te	S	Au	Ag	
G-1C 3_5	0.27	0.74		0.98	0.01	
G-1D 12_12	0.33	0.70	0.003	0.97	0.01	
G-1D 12_16	0.34	0.69	0.001	0.97	0.01	
G-1D 12_11	0.34	0.69	0.001	0.96	0.01	
G-1D 12_13	0.34	0.69	0.002	0.96	0.01	
G-1D 12_15	0.34	0.68	0.001	0.96	0.01	
G-1D 12_14	0.35	0.68	0.001	0.96	0.01	
G-1C 3_3	0.38	0.63	0.001	0.96	0.02	
G-1C 3_1	0.38	0.63	0.001	0.96	0.02	
G-1C 3_6	0.50	0.52	0.001	0.97	0.01	
2a	0.25	0.76		0.97	0.02	
2b	0.25	0.77		0.96	0.02	
3a	0.38	0.66		0.94	0.02	
3b	0.38	0.66		0.95	0.02	
4a	0.48	0.55		0.95	0.03	
4b	0.49	0.55		0.94	0.03	
6a	0.47	0.56		0.96	0.02	
6b	0.47	0.55		0.96	0.02	
Average	0.37	0.65	0.001	0.96	0.02	

*The 18 EPMA results correspond to gachingite formula: $(Au_{0.96}Ag_{0.02})_{\Sigma 0.98}(Te_{0.65}Se_{0.37})_{\Sigma 1.02}$. Grains 3 and 4 were used for Raman analyses and grains 3 and 6 for EBSD measurements.

https://doi.org/10.1180/mgm.2022.9 Published online by Cambridge University Press

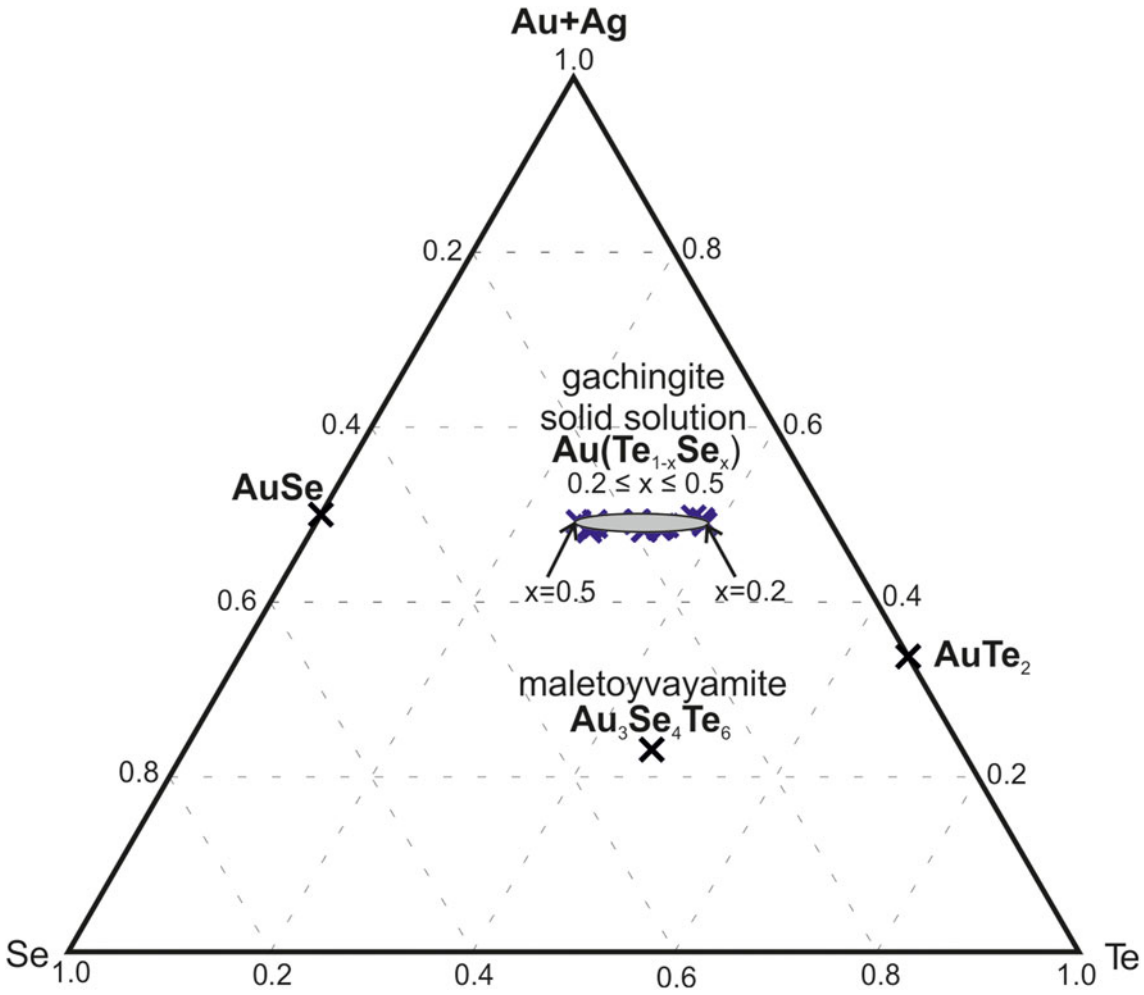

Fig. 4. EPMA data for gachingite, plotted in the Au–Te–Se diagram.

were classified as unique with $I > 3\sigma(I)$. Corrections for background, Lorentz effects and polarisation were applied during the data reduction in the Rigaku program *CrysAlis*. The crystal structure was solved with the charge-flipping method using the program *Superflip* (Palatinus and Chapuis, 2007) and subsequently refined by the full-matrix least-squares algorithm of *Jana2006* program (Petříček *et al.*, 2014). The crystal structure solution indicated one independent Au position (8*e*) and one Se/Te mixed position (8*f*) in the *Cmce* space group. The refinement of Se/Te position yielded 0.468(10) and 0.532(10) occupancy factors for Se and Te, respectively. All atoms were refined with anisotropic displacement parameters. Final refinement for 13 parameters converged to $R = 0.0182$ and $wR = 0.0390$ for 229 independent reflections. Details of data collection, crystallographic data, and refinement for the synthetic analogue of gachingite are given in Table 3. Table 4 and Table 5 show atomic positions and anisotropic displacement parameters, respectively. The crystallographic information file has been deposited with the Principal Editor of *Mineralogical Magazine* and is available as Supplementary material (see below).

Powder X-ray diffraction data of synthetic analogue of gachingite $Au_{1.00}(Te_{0.50}Se_{0.50})$ were collected in Bragg-Brentano geometry using a Bruker D8 Advance powder diffractometer. Nickel filtered Cu*K*α radiation was used, a 10 mm automatic divergence slit and a Lynx EyeXE detector. Data were collected in the angular range from 10 to 140° of 2θ with a 0.01° step. Refined unit-cell parameters of synthetic $Au_{1.00}(Te_{0.50}Se_{0.50})$ are the following: $a = 7.5569(2)$ Å, $b = 5.7448(1)$ Å, $c = 8.9253(2)$ Å and $V = 387.47(1)$ Å^3. Powder X-ray diffraction data are given in Table 6.

Structure description

The framework crystal structure of gachingite (Fig. 5) contains one crystallographically independent Au and one Se/Te mixed position (0.468/0.532 occupancy parameters). Au is almost linearly coordinated by two Se/Te atoms at 2.526 Å. The Se/Te–Au–Se/Te bonding angle is 166.10° instead of 180° for perfect linear coordination. The Au shows the additional two Au contacts at 2.87 Å, which is comparable to that of 2.88 Å found in native gold by Straumanis (1971), indicating strong Au–Au interaction in the gachingite structure. As is evident in Fig. 5b, Au atoms form [Au–Au–Au] chains oriented along the **b**-axis. Se/Te atoms form a group $(Se/Te)_2^{-2}$, with a strong covalent Se/Te–Se/Te bond with a distance of 2.526 Å. The Se/Te atoms are further coordinated by two Au atoms at 2.526 Å, forming trigonal pyramidal coordination. These three short bonds are accompanied by two considerably longer Te/Se–Au contacts (3.471 Å). This asymmetric coordination of Se/Te atoms might suggest the

https://doi.org/10.1180/mgm.2022.9 Published online by Cambridge University Press

Table 3. Single-crystal data collection and structure refinement details for synthetic analogue of gachingite, $Au_{1.00}(Te_{0.50}Se_{0.50})$.

Crystal data	
Structural formula	$Au_{1.00}(Te_{0.532}Se_{0.468})$
Space group	*Cmce* (64)
Unit cell dimensions (Å)	
	$a = 7.5379(12)$
	$b = 5.7415(10)$
	$c = 8.8985(13)$
V (Å^3)	385.12(11)
Z	8
Density (for above formula) (g·cm^{-3})	10.41
Absorption coefficient (mm^{-1})	92.588
Data collection	
Diffractometer	Rigaku SuperNova with Atlas S2 CCD
X-ray radiation/power	Mo$K\alpha$ ($\lambda = 0.71075$ Å)/ 40 kV, 30 mA
Temperature (K)	297 K
Crystal size (μm)	17 × 12 × 7
F(000)	981
θ range (°)	4.58 to 29.34°
Index ranges	$-9 \le h \le 9$, $-6 \le k \le 7$, $-12 \le l \le 8$
Reflections collected/unique	1109/266
Reflections with $I > 3\sigma I$	229
Completeness to θ = 25.03°	
Refinement	
Refinement method	Full-matrix least-squares on F^2
R_{int}	0.0254
Parameter/restraints/constraints	13/0/0
GoF	1.10
Final R indices [$I > 3\sigma I$]	$R = 0.0182$, $wR = 0.0390$
R indices (all data)	$R = 0.0242$, $wR = 0.0420$
Weighting scheme, Weights	Based on measured s.u.'s, $w = 1/(\sigma^2(I) + 0.000256I^2)$
Largest diff. peak/hole (e$^-$·Å^{-3})	+1.00, −1.53

Table 4. Atom coordinates and equivalent displacement parameters (Å^2) for the synthetic analogue of gachingite, $Au_{1.00}(Te_{0.50}Se_{0.50})$.

Atom	Wyckoff position	Occupancy	x	y	z
Au	8*e*	1	¼	0.65144(7)	¼
Se	8*f*	0.468(10)	½	0.70468(14)	0.43591(12)
Te	8*f*	0.532(10)	½	0.70468(14)	0.43591(12)

Table 6. Powder X-ray diffraction data (Cu$K\alpha$, Bragg-Brentano geometry) for the synthetic analogue of gachingite, $Au_{1.00}(Te_{0.50}Se_{0.50})$.*

I_{obs}	I_{calc}	d_{obs}	d_{calc}	h	k	L
65	**56**	**4.461**	**4.462**	**0**	**0**	**2**
8	7	4.070	4.070	1	1	1
11	7	3.777	3.778	2	0	0
36	**30**	**3.194**	**3.194**	**1**	**1**	**2**
99	**96**	**2.883**	**2.883**	**2**	**0**	**2**
100	**100**	**2.734**	**2.734**	**0**	**2**	**1**
33	**24**	**2.231**	**2.231**	**0**	**0**	**4**
51	**43**	**2.215**	**2.215**	**2**	**2**	**1**
21	18	2.066	2.066	0	2	3
6	5	2.046	2.049	3	1	2
26	21	2.035	2.035	2	2	2
20	18	2.005	2.005	1	1	
28	**23**	**1.921**	**1.921**	**2**	**0**	**4**
14	12	1.889	1.889	4	0	0
8	7	1.817	1.817	1	3	1
63	**57**	**1.813**	**1.813**	**2**	**2**	**3**
3	2	1.762	1.762	0	2	4
4	4	1.740	1.739	4	0	2
3	3	1.714	1.713	1	3	2
6	6	1.604	1.603	3	1	4
5	4	1.579	1.578	4	2	0
1	1	1.575	1.574	1	3	3
18	16	1.554	1.554	4	2	1
22	21	1.516	1.516	0	2	5
3	2	1.436	1.436	0	4	0
9	7	1.418	1.418	0	4	1
3	2	1.414	1.414	1	1	6
9	8	1.407	1.407	2	2	5
5	5	1.394	1.394	4	2	3
4	3	1.384	1.384	2	0	6
9	9	1.367	1.367	0	4	2
9	8	1.342	1.342	2	4	0
3	3	1.327	1.327	2	4	1
4	4	1.321	1.321	0	2	6
4	2	1.285	1.285	2	4	2
14	13	1.223	1.224	2	4	3
4	4	1.207	1.208	0	4	4
10	10	1.182	1.182	4	2	5
6	6	1.169	1.168	4	0	6
4	4	1.166	1.165	0	2	7
5	5	1.150	1.150	2	4	4
2	2	1.126	1.127	1	5	1
5	5	1.119	1.119	0	4	5
10	8	1.114	1.114	2	2	7
9	8	1.070	1.070	2	0	8

*Strongest lines are given in bold.

stereoactivity of lone electron pairs at Se and Te atoms. Considering the $(Se/Te)_2^{-2}$ group, the gachingite chemical formula can be alternatively written as $Au_2(Se/Te)_2$. Au shows an oxidation state of + I and not +II. This agrees with the approximately linear coordination of Au in gachingite, which is typical for Au^{+1} with d^{10} electronic configuration (Rabenau and Schulz, 1976; Schutte and de Boer, 1988).

It is interesting to note that the presence of [Au–Au–Au] chains with the strong Au–Au bonds in the crystal structure of gachingite points to a special group of materials, which are known as 'one-dimensional metals'. Such materials show metallic conductivity in one direction and do not possess metallic conductivity in perpendicular directions (i.e. conductivity is strongly anisotropic). This phenomenon requires strong orbital overlap on neighbouring atoms within a chain and negligible interaction between chains. Whereas the first condition is met in the gachingite structure (i.e. strong Au–Au bonds), the second is only partially fulfilled (i.e. interconnections of chains by Se(Te) atoms). Nevertheless, the 1D-character of metallic bonds is a hallmark of the gachingite crystal structure. Gachingite forms a limited solid-solution from $Au(Te_{0.5}Se_{0.5})$ to $Au(Te_{0.8}Se_{0.2})$, where Se–Te substitution occurs. Its stability field does not include the AuSe phase. Both Se and Te atoms are essential for gachingite

Table 5. Anisotropic displacement parameters (Å^2) for the synthetic analogue of gachingite, $Au_{1.00}(Te_{0.50}Se_{0.50})$.

Atom	U^{11}	U^{22}	U^{33}	U^{12}	U^{13}	U^{23}	U_{eq}
Au	0.00215(3)	0.0131(2)	0.0191(3)	0	−0.0013(2)	0	0.01791(17)
Se/Te	0.01765(5)	0.0157(4)	0.0168(6)	0	0	−0.0004(4)	0.0167(3)

https://doi.org/10.1180/mgm.2022.9 Published online by Cambridge University Press

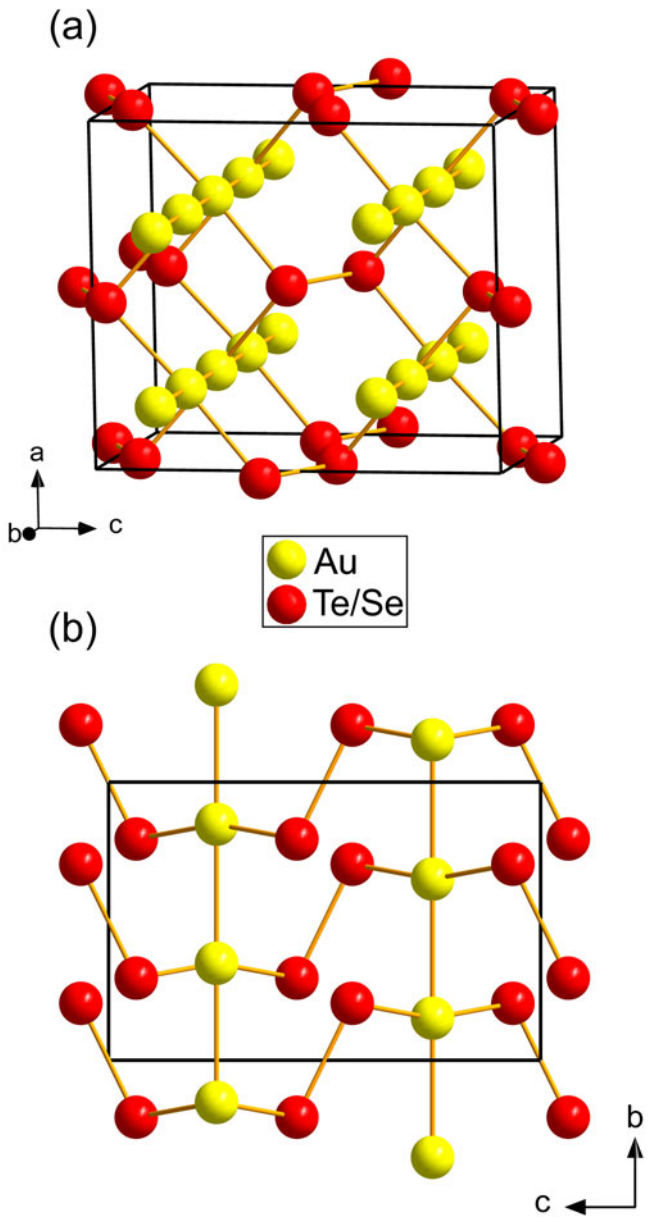

Fig. 5. Crystal structure of the synthetic analogue of gachingite, $Au_{1.00}(Te_{0.50}Se_{0.50})$. Note the [Au–Au–Au] chains oriented along the **b**-axis.

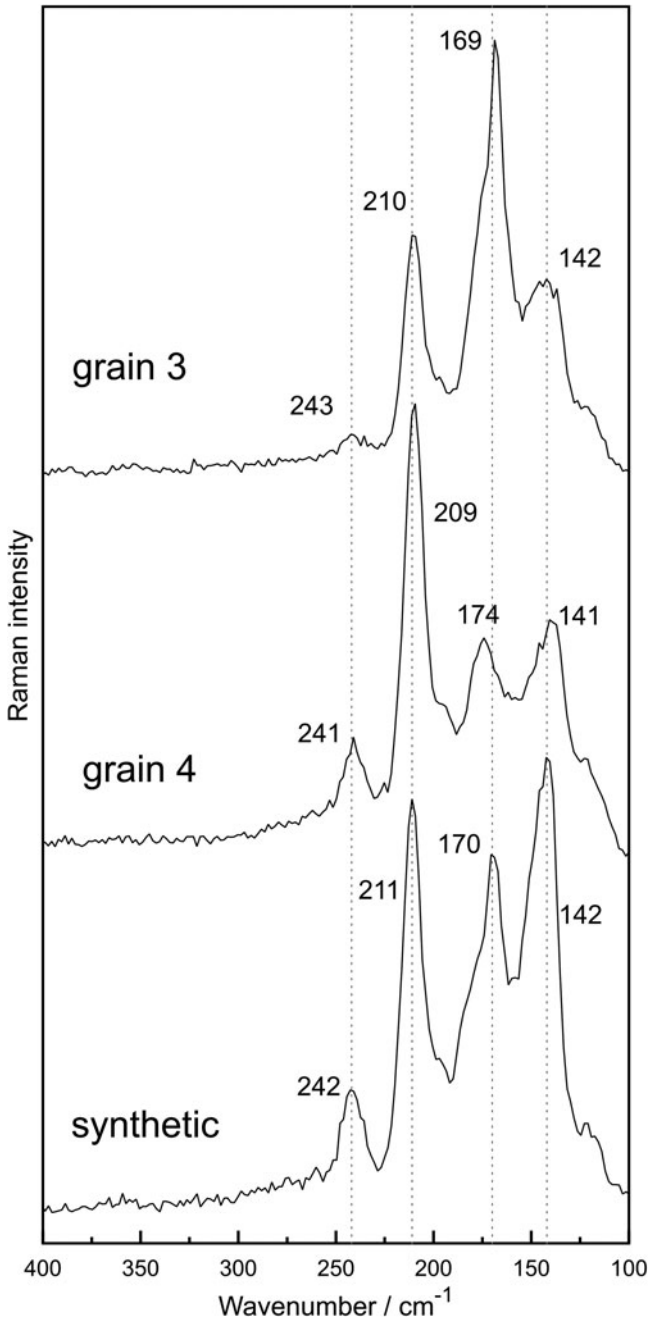

Fig. 6. Raman spectra of gachingite in comparison with its synthetic analogue, $Au_{1.00}(Te_{0.50}Se_{0.50})$.

formation. Crystal structure analysis confirms the Se/Te mixed position; no indication of Se and Te ordering has been observed. Therefore, we have chosen $Au(Te_{1-x}Se_x)$, $0.2 \approx x \leq 0.5$ ($Z = 8$) as the simplified chemical formula of gachingite. It is interesting to note that an orthorhombic Au_2SeTe phase with $Z = 4$ and similar unit-cell parameters to gachingite was synthesised by Cranton and Heyding (1968). However, no crystal structure analysis was performed at that time. It is worth noting that the crystal structure of maletoyvayamite $Au_3Se_4Te_6$ (Tolstykh *et al.*, 2020), another ternary phase from the Au–Se–Te system, is based on molecular $[Au_6Se_8Te_{12}]$ clusters and hence differs considerably from that of gachingite. Another distinction between these two mineral species concerns the Au coordination by chalcogen atoms. Though Au is linearly coordinated in the gachingite, the maletoyvayamite structure contains $[AuTe_4]$ squares. On the other hand, both structures contain covalent Se–Te bonds indicating relatively high stability of these atomic interactions in the Au–Se–Te system.

Raman spectroscopy

The spectroscopic investigation of gachingite was carried out using a Renishaw inVia Reflex Raman system coupled with a Leica microscope. Individual grains of gachingite were measured with a 100× objective lens with excitation provided by a 514.5 nm Ar-ion laser and the signal was recorded by a thermoelectrically cooled CCD detector (100–4000 cm^{-1} spectral wavenumber, the spectral resolution of 2 cm^{-1}). To achieve an enhanced signal-to-noise ratio, 30 scans were accumulated, each 20 s exposure

https://doi.org/10.1180/mgm.2022.9 Published online by Cambridge University Press

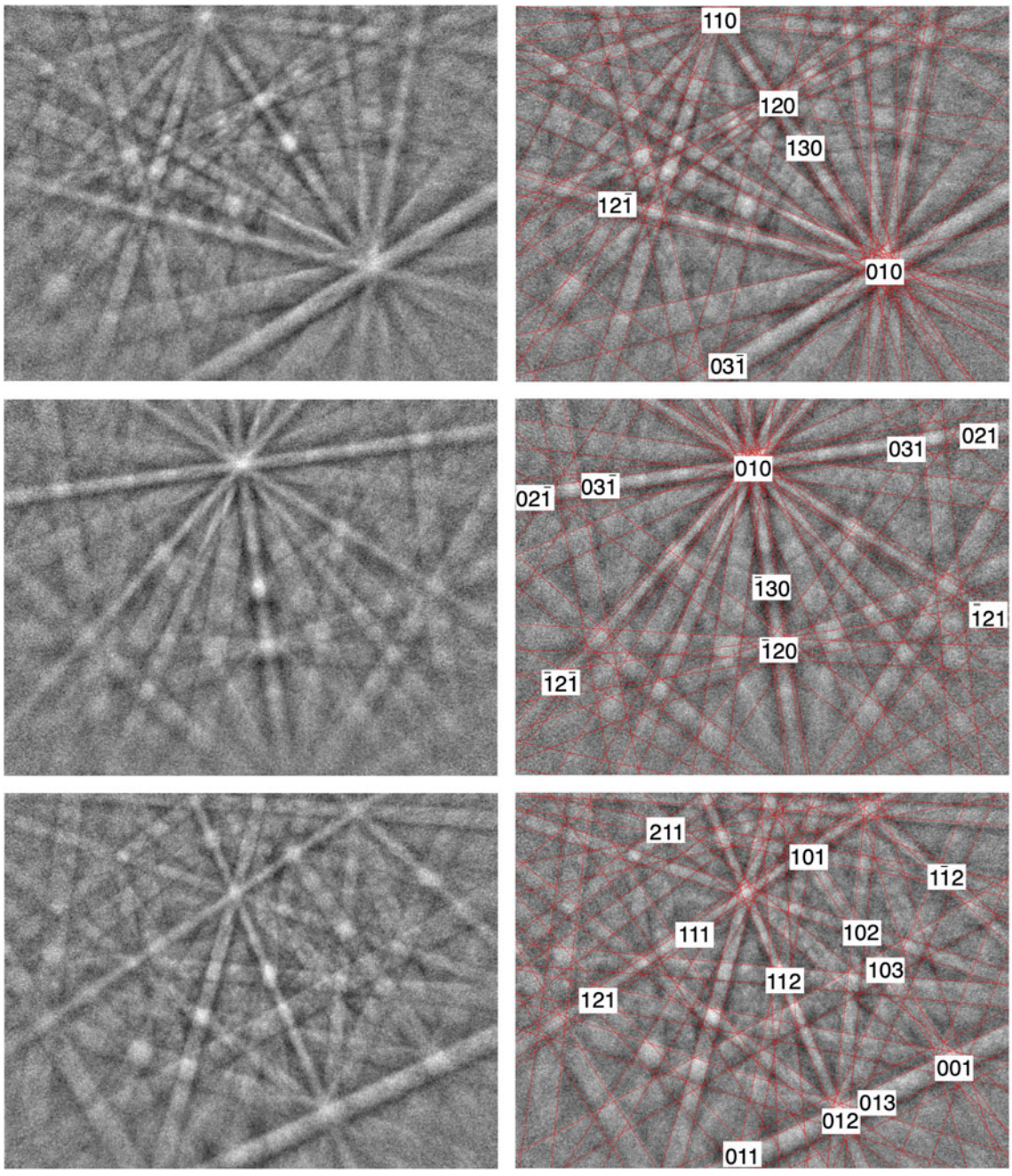

Fig. 7. EBSD images of gachingite at the different grain orientations; in the right pane, the Kikuchi bands are indexed.

time, with laser power at the source, kept at a maximum of 2 mW to avoid thermal degradation. A polystyrene standard was used to check the wavenumber calibration and the spectra obtained were analysed using the *GRAMS/AI 9.1* software package (Thermo Fisher scientific).

Raman spectra were measured for two distinct gachingite grains (Fig. 6, labelled as grain 3 and 4) and the synthetic analogue. The following intense bands were observed at 142, 169, 210 and 243 cm^{-1} for grain 3; and 141, 174, 209 and 241 cm^{-1} for grain 4. Almost identical bands were also observed for the synthetic analogue: 142, 170, 211 and 242 cm^{-1}. The obtained spectra are shown in Fig. 6. Interestingly, the intensities of bands are slightly different for both natural grains and synthetic counterparts. Otherwise, the bands are well-resolved, and the spectra are very distinct from maletoyvayamite (Tolstykh *et al.*, 2020). Similar spectral shapes are reported for Se–Te glasses as well as Se–Te mixed crystals where the dominant spectral features are attributed to the Se–Se, Se–Te, and Te–Te vibrations in the 100–300 cm^{-1} region (Geick *et al.*, 1972, Tverjanovich *et al.*, 2018). The observed Raman bands are therefore tentatively assigned to the Se–Se, Se–Te and Te–Te vibrations, however the contribution of Au–Te/Se vibrations can also be considered. The intensity changes and small shifts probably arise due to the variable content of Te and Se in the measured grains. The Raman spectra of gachingite and its synthetic analogue $Au_{1.00}(Te_{0.50}Se_{0.50})$ are in agreement and further supports the structural identity between synthetic and natural material.

https://doi.org/10.1180/mgm.2022.9 Published online by Cambridge University Press

Electron back-scatter diffraction (EBSD)

A TESCAN Mira 3GMU scanning electron microscope combined with an electron back-scatter diffraction (EBSD) system (NordlysNano detector, Oxford Instruments), the Czech Geological Survey, was used on gachingite. The polished section surface was polished using OP-S colloidal silica and subsequently carbon-coated, ca. 10 nm thick. The EBSD patterns collected on gachingite (25 spot analyses) were found to match those calculated based on the refined structural model for synthetic $Au_{1.00}(Te_{0.50}Se_{0.50})$ (Fig. 7). The values of the mean angular deviation (MAD, i.e. the goodness of fit of the solution) between the calculated and measured Kikuchi bands range between 0.14° and 0.45°. These values reveal a very good match; if values of mean angular deviation are <1°, they are considered as indicators of an acceptable fit (HKL Technology, 2004). The EBSD measurements further support the structural identity between gachingite and its synthetic analogue.

Acknowledgements. This paper is dedicated to Evgenyi G. Sidorov (1955–2021), without whom the fieldwork, collection of samples and finding of this mineral at Kamchatka would not be possible. Unfortunately, he passed away before the mineral was accepted by the IMA–CNMNC. The authors acknowledge Ritsuro Miyawaki, Chairman of the CNMNC of IMA and its members for helpful comments on the submitted data. We thank the Principal Editor Stuart Mills, Structural Editor Peter Leverett, Igor V. Pekov and one anonymous reviewer. The authors are grateful to E. Petrova (RPE "Ekekhim") and N. Stenin (Lead metallurgist and Interminerals LLC) for the samples provided for this study. The studies were carried out within the framework of the state assignment of the IGM SB RAS financed by the Ministry of Science and Higher Education of the Russian Federation and the Czech Geological Survey, Czech Republic. The authors would like to thank V. Korolyuk and M. Khlestov (IGM SB RAS), O. Pour (Czech Geological Survey) and Z. Korbelová (Czech Academy of Sciences) for the WDS and EDS analyses and L. Vrtiška (National Museum in Prague) for reflectance measurements. This research was supported by the Russian Foundation of Basic Research projects No 19-05-00316, by the Grant Agency of the Czech Republic (project No. 22-26485S), by the Strategic Research Plan of the Czech Geological Survey (DKRVO/ČGS 2018–2022) and by institutional funding from the Center for Geosphere Dynamics (UNCE/SCI/006). We acknowledge CzechNanoLabResearch Infrastructure supported by MEYS CR (LM2018110) for financial support for the collection of diffraction data.

Supplementary material. To view supplementary material for this article, please visit https://doi.org/10.1180/mgm.2022.9

References

Cranton G.E. and Heyding R.D. (1968) The gold/selenium system and some gold seleno-tellurides. *Canadian Journal of Chemistry*, **46**, 2637–2640.

Geick R., Steigmeier E.F. and Auderset H. (1972) Raman effect in selenium-tellurium mixed crystals. *Physica Status Solidi B*, **54**, 623–630.

Goryachev N.A., Volkov A.V., Sidorov A.A., Gamyanin G.N., Savva N.Y. and Okrugin V.M. (2010) Au-Ag-mineralization of volcanogenic belts of the northeast Asia. *Lithosphere*, **3**, 36–50 [In Russian].

HKL Technology (2004) *Channel* 5. HKL–Technology A/S, Hobro, Denmark

Khanchuk A.I. and Ivanov V.V. (1999) Meso-Cenozoic geodynamic settings and gold mineralization of the Russian Far East. *Russian Geology and Geophysics*, **40**, 1607–1617.

Lavrent'ev Yu.G., Karmanov N.S. and Usova L.V. (2015) Electron probe microanalysis of minerals: microanalyzer or scanning electron microscope? *Russian Geology and Geophysics*, **8**, 1154–1161.

Lyashenko L.L. and Mikhaylova G.N. (1972) *Report on the results of exploration work within the Maletoyamyam sulfur ore cluster*. Enyngvayamskaya PDP, 1970–1971, foundations [in Russian].

Melkomukov B.H., Razumny A.V., Litvinov A.P. and Lopatin W.B. (2010) The new highly promising gold objects of Koryakiya. *Mining Bulletin of Kamchatka*, **14**, 70–74 [In Russian].

Okrugin V., Kokarev S., Okrugina A., Chubarov V. and Shuvalov R. (1994) An unusual example of the interaction of modern hydrothermal system with Au-Ag veins (Southern Kamchatka). *Mineralogical Magazine*, **58A**, 669–670 [Goldschmidt abstract].

Okrugin V.M., Shishkanova K.O. and Yablokova D.A. (2015) About the ores of the Amethystovoe deposits (Kamchatka). *Mining Bulletin of Kamchatka*, **3–4**, 33–34 [In Russian].

Okrugin V., Shishkanova K. and Philosophova T. (2017) New data on ores from the Vilyuchinskoe Au-Ag polymetallic ore occurrence, South Kamchatka. *Ore and Metals*, **1**, 40–54 [In Russian].

Palatinus L. and Chapuis G. (2007) SUPERFLIP—A computer program for the solution of crystal structures by charge flipping in arbitrary dimensions. *Journal of Applied Crystallography*, **40**, 786–790.

Petříček V., Dušek M., and Palatinus L. (2014) Crystallographic Computing System JANA2006: General features. *Zeitschrift für Kristallographie* **229**, 345–352.

Rabenau A. and Schulz H. (1976) The crystal structure of α-AuSe and β-AuSe. *Journal of the Less-Common Metals* **48**, 89–101.

Schutte W.J. and de Boer J.L. (1988) Valence fluctuations in the incommensurately modulated structure of calaverite $AuTe_2$. *Acta Crystallographica*, **B44**, 486–494.

Shapovalova M., Tolstykh N. and Bobrova O. (2019) Chemical composition and varieties of sulfosalts from gold mineralization in the Gaching ore occurrence (Maletoyvayam ore field). *IOP Conf. Series: Earth and Environmental Science*, **319**, 012019.

Sidorov E.G., Borovikov A.A., Tolstykh N.D., Bukhanova D.S., Palyanova G.A. and Chubarov V.M. (2020) Gold mineralization at the Maletoyvayam deposit (Koryak Highland, Russia) and physicochemical conditions of its formation. *Minerals*, **10**, 1093.

Straumanis M.E. (1971), Neubestimmung der Gitterparameter, Dichten und thermischen Ausdehnungskoeffizienten von Silber und Gold, und Vollkommenheit der Struktur. *Monatshefte fuer Chemie*, **102**, 1377–1386.

Takahashi R., Matsueda H. and Okrugin V.M. (2002) Hydrothermal gold mineralization at the Rodnikovoe deposit in South Kamchatka, Russia. *Resource Geology*, **52**, 359–369.

Takahashi R., Matsueda H., Okrugin V.M. and Ono S. (2007) Epithermal gold-silver mineralization of the Asachinskoe deposit in South Kamchatka, Russia. *Resource Geology*, **57**, 354–373.

Tolstykh N., Vymazalová A., Petrova E. and Stenin N. (2017) The Gaching Au mineralization in the Maletoyvayam ore field, Kamchatka, Russia. Pp. 195–198 in: *Materials Mineral Resources to Discover*. Proceedings of the 14th Biennial SGA Meeting, 17–20 August 2017, Quebec City, Canada, Vol. 1.

Tolstykh N., Vymazalová A., Tuhý M., and Shapovalova M. (2018) Conditions of Au-Se-Te mineralization in the Gaching ore occurrence (Maletoyvayam ore field), Kamchatka, Russia. *Mineralogical Magazine*, **82**, 649–674.

Tolstykh N., Palyanova G., Bobrova O. and Sidorov E. (2019) Mustard gold of the Gaching ore occurrence (Maletoyvayam deposit, Kamchatka, Russia). *Minerals*, **9**, 489.

Tolstykh N.D., Tuhý M., Vymazalová A., Plášil J., Laufek F., Kasatkin A.V., Nestola F. and Bobrova O.V. (2020) Maletoyvayamite, $Au_3Se_4Te_6$, a new mineral from Maletoyvayam deposit, Kamchatka peninsula, Russia. *Mineralogical Magazine*, **84**, 117–123.

Tolstykh N., Tuhý M., Vymazalová A., Plášil J., Laufek F., Košek F. and Sidorov E.G. (2021) Gachingite, IMA 2021-008. CNMNC Newsletter No. 62. *Mineralogical Magazine*, **85**, 634–638.

Tsukanov N. (2015) Tectono-stratigraphic terranes of Kamchatka active margins: structure, composition and geodynamics. Pp. 97–103 in: *Materials of the Annual conference "Volcanism and Related Processes"*. Petropavlovsk-Kamchatsky, Kamchatka Krai, Russia [in Russian].

Tverjanovich A., Cuisset A., Fontanari D. and Bychkov E. (2018) Structure of Se–Te glasses by Raman spectroscopy and DFT modeling. *Journal of the American Ceramic Society*, **101**, 5188–5197.